RSC Advances

PAPER

View Article Online
View Journal | View Issue

Cite this: *RSC Adv.*, 2023, **13**, 7503

Triterpenoid saponins and C_{21} steroidal glycosides from *Gymnema tingens* and their glucose uptake activities†

Jinhua He,[a] Ping Tang,[bc] Meiyu Liu,[a] Guangfeng Liao,[a] Rumei Lu*[a] and Xinzhou Yang *[ab]

Received 11th November 2022
Accepted 21st February 2023

DOI: 10.1039/d2ra07164a

rsc.li/rsc-advances

Four new triterpenoid saponins, tigensides A–D (**1–4**), and one new C_{21} steroid, tipregnane A(**9**), together with six known compounds were isolated from the EtOAc fraction of the roots and stems of *Gymnema tingens*. The chemical structures of the new compounds were determined based on their spectroscopic data, including IR, UV, NMR, and mass spectrometric analysis. All compounds were isolated for the first time. Compounds **1–11** promoted glucose uptake in the range of 1.12 to 2.52 fold, respectively. Compound **2** showed the most potent glucose uptake, with 2.52 fold enhancement. Additionally, compound **2** showed a medium effect on the GLUT4 translocation activity in L6 cells in further study.

Introduction

Diabetes mellitus (DM) is a metabolic chronic disease characterized by hyperglycemia and insulin resistance (IR), which is caused by a lack of insulin secretion or insulin response.[1] In 2017, approximately, 425 million people (1 in 11 adults) were affected with diabetes and this may rise to 693 million in 2045.[2] Type 2 DM (T2DM) accounts for 90–95% of global diabetes.[3] The treatment of diabetes accounts for around 12% of overall global health-care expenditures with respect to socioeconomic burden.[4] Current synthetic agents and insulin used effectively for the treatment of diabetes are scarce and expensive with prominent adverse effects. Natural products and their active ingredients have advantages such as minimal side effects, being rich in resources, and low price. Therefore, the complementary and alternative approach to screen new effective hypoglycemic drugs through isolation of phytochemicals from natural products is imperative[5,6]

The genus *Gymnema* of the family Asclepiadaceae comprises 25 species, which are distributed in tropical region of Asia, and subtropical regions of southern Africa and Oceania.[7] Previous phytochemical studies on *Gymnemas* have led to the isolation and identification of triterpenoids, triterpenoid saponins, C_{21} steroids, C_{21} steroidal glycosides, flavonoids, peptides, polysaccharides and several other components.[8–14] All of the components described above play an important role related to several bioactivities, such as anti-diabetic, anti-inflammatory, anti-bacterial, anti-arthritic, anti-hyperlipidemic, cytotoxic, and immunostimulatory activities.[15–21] Some triterpenoid saponins from the genus *Gymnema* were found to be able to attenuate hyperglycemia induced by pituitary growth hormone or adrenocorticotropic hormone and to inhibit intestinal glucose absorption in diabetic rats.[22–27] In traditional herbal medicine, the *Gymnema* species has been well known for the anti-diabetic potential.[28]

Gymnema tingens Spreng. is a plant of the genus *Gymnema*. In China, it is distributed in the provinces of Guangdong, Guangxi, Guizhou and Yunnan, and grows in hillsides, forests or shrubs. It is a folklore medicine in China used for the treatment of rheumatism and polio.[29] Previous phytochemical studies on *Gymnema tingens* have led to the isolation and identification of triterpenoids, steroids, phenolic glycosides, and several other components.[30–32] However, few studies have been reported on its bioactive components with respect to possible antidiabetic activity. In our previous investigation, we found that the EtOAc fraction of *G. tingens* showed a good activity on glucose uptake. As part of an ongoing search for bioactive compounds from *Gymnema* plants, we performed purification of the EtOAc fraction of *G. tingens* by chromatography column and semi-preparative phase HPLC, and obtained four new triterpenoid saponins, tigensides A–D (**1–4**), and one new C_{21} steroid, tipregnane A (**9**), together with six known compounds. The structures were identified by spectroscopic analysis and comparison of observed and reported spectroscopic data.

In addition, we tested the glucose uptake activity of compounds **1–11** and the GLUT4 translocation activity of compound **2** in L6 cells in the further study. As the important

[a]*College of Pharmacy Guangxi University of Chinese Medicine, Nanning 530200, China. E-mail: lrm1969@163.com*

[b]*School of Pharmaceutical Sciences, South-Central Minzu University, Wuhan 430074, China. E-mail: xzyang@mail.scuec.edu.cn*

[c]*Key Laboratory of the Ministry of Education of Xinjiang Phytomedicine Resources Utilization, Pharmacy School of Shihezi University, Shihezi 832002, Xinjiang, P. R. China*

† Electronic supplementary information (ESI) available. See DOI: https://doi.org/10.1039/d2ra07164a

Table 1 ^{1}H-NMR (600 MHz) data for compounds **1–4** and **9** (J in Hz)

	δ_H (J in Hz)				
No.	**1**[a]	**2**[a]	**3**[a]	**4**[a]	**9**[b]
1	1.44 (m)/0.87 (m)	1.42 (m)/0.86 (m)	1.40 (m)/0.86 (m)	1.39 (m)/0.85 (m)	1.15 (m)/1.90 (m)
2	2.18 (m)/1.88 (m)	2.17 (m)/1.87 (m)	2.15 (m)/1.86 (m)	2.15 (m)/1.85 (m)	1.55 (m)/1.82 (m)
3	3.38 (dd, 11.8, 4.4)	3.39 (dd, 12.1, 4.5)	3.36 (dd, 11.8, 4.4)	3.36 (dd, 11.8, 4.0)	3.60 (m)
4					2.38 (m)/2.41 (m)
5	0.79 (m)	0.78 (m)	0.79 (m)	0.78 (m)	
6	1.49 (m)/1.31 (m)	1.49 (m)/1.30 (m)	1.48 (m)/1.30 (m)	1.47 (m)/1.29 (m)	5.67 (d, 4.7)
7	1.57 (m)/1.34 (m)	1.50 (m)/1.26 (m)	1.56 (m)/1.32 (m)	1.56 (m)/1.33 (m)	4.06 (d, 5.2)
8					
9	1.59 (m)	1.56 (m)	1.59 (m)	1.58 (m)	1.82 (m)
10					
11	1.83 (m)	1.84 (m)/1.80 (m)	1.80 (m)	1.80 (m)	1.84 (m)/2.02 (m)
12	5.37 (brs)	5.42 (brs)	5.35 (brs)	5.35 (brs)	4.86 (overlapped)
13					
14					
15	2.20 (d, 12.2)/1.26 (m)	2.11 (m)/1.67 (m)	2.16 (m)/1.72 (m)	2.15 (m)/1.73 (m)	2.32 (m)
16	5.11 (dd, 11.5, 5.2)	5.15 (dd, 11.1, 5.2)	5.17 (dd, 11.5, 5.3)	5.19 (overlapped)	2.07 (m)
17					
18	3.05 (d, 13.5)	3.16 (dd, 11.1, 4.3)	2.95 (dd, 13.9, 4.6)	2.96 (dd, 14.0, 3.5)	1.64 (s)
19	2.00 (m)/1.26 (m)	2.28 (m)/1.39 (m)	2.05 (m)/1.23 (m)	2.05 (m)/1.23 (m)	1.14 (s)
20					4.91 (d, 6.2)
21	2.00 (m)	5.89 (d, 11.3)	2.11 (m)/1.96 (m)	2.10 (m)/1.97 (m)	1.36 (d, 6.2)
22	6.37 (dd, 10.9, 5.1)	6.51 (d, 11.2)	4.86 (overlapped)	4.87 (dd, 11.6, 2.3)	
23	1.33 (s)	1.34 (s)	1.32 (s)	1.32 (s)	
24	1.00 (s)	1.00 (s)	0.97 (s)	0.98 (s)	
25	0.82 (s)	0.81 (s)	0.82 (s)	0.82 (s)	
26	0.95 (s)	0.90 (s)	1.13 (s)	1.11 (s)	
27	1.45 (s)	1.40 (s)	1.43 (s)	1.43 (s)	
28	4.51 (m)/4.09 (d, 10.6)	4.36 (d, 10.8)/4.09 (d, 10.9)	5.35 (m)/4.89 (d, 10.9)	5.43 (d, 10.8)/4.95 (d, 11.1)	
29	1.01 (s)	1.07 (s)	1.04 (s)	1.05 (s)	
30	1.30 (s)	1.34 (s)	1.17 (s)	1.17 (s)	
	Anth	Anth	Anth	Bz	Cin
1′					
2′					6.11 (d, 16.0)
3′				8.26 (dd, 7.8, 2.4)	7.45 (d, 16.0)
4′	6.67 (dd, 7.8, 1.2)	6.64 (dd, 8.4, 1.8)	6.66 (dd, 8.4, 1.2)	7.45 (t, 7.8)	
5′	7.39 (ddd, 7.8, 7.2, 1.8)	7.36 (ddd, 8.4, 8.1, 1.2)	7.42 (ddd, 8.4, 7.8, 1.5)	7.53 (t, 7.8)	7.28 (d, 7.2)
6′	6.66 (ddd, 8.4, 7.2, 1.2)	6.60 (ddd, 8.1, 7.8, 1.8)	6.71 (ddd, 8.0, 7.8, 1.2)	7.45 (t, 7.8)	7.33 (m)
7′	8.48 (dd, 8.4, 1.8)	8.46 (dd, 7.8, 1.2)	8.26 (dd, 8.0, 1.5)	8.26 (dd, 7.8, 2.4)	7.37 (m)
8′	2.80 (overlapped)	2.75 (overlapped)	2.64 (overlapped)		7.33 (m)
9′	8.40 (m)	8.17 (m)	7.99 (m)		7.28 (d, 7.2)

Table 1 (*Contd.*)

	Glucuronopyranosyl methyl ester	Glucuronopyranosyl methyl ester	Glucuronopyranosyl methyl ester	Glucuronopyranosyl methyl ester	B_Z
1″	5.03 (d, 7.8)	5.04 (d, 7.8)	5.01 d (7.8)	5.01 d (7.8)	
2″	4.14 (dd, 9.0, 7.8)	4.14 (dd, 9.0, 7.8)	4.12 (dd, 9.0, 7.8)	4.12 (dd, 9.0, 7.8)	
3″	4.31 (dd, 9.6, 9.0)	4.31 (dd, 9.6, 9.0)	4.30 (dd, 9.6, 9.0)	4.30 (dd, 9.6, 9.0)	7.92 (dd, 7.2, 1.5)
4″	4.52 (dd, 9.7, 9.6)	4.52 (dd, 9.7, 9.6)	4.51 (dd, 9.7, 9.6)	4.51 (dd, 9.7, 9.6)	7.36 (m)
5″	4.64 (d, 9.7)	4.65 (d, 9.7)	4.63 (d, 9.7)	4.63 (d, 9.7)	7.56 (t, 7.2)
6″					7.36 (m)
7″	3.75, s	3.75, s	3.75, s		7.92 (dd, 7.2, 1.5)
			Ac		
1‴					
2‴		1.89 (s)			

[a] Pyridine-d_5 as solvent. [b] $CDCl_3$ as solvent.

protein for preserving whole-body glucose homeostasis, GLUT4 is considered to be a potential therapeutic target for the treatment of T2DM.[33] Herein, we report the isolation and structure elucidation of these isolated compounds, as well as their biological activities. These results suggest that the *G. tingens* have the potential to become a source for new antidiabetic drug discovery.

Results and discussion

Structural elucidation of the isolated compounds

Compound **1** was isolated as a yellow, amorphous powder with an $[\alpha]_D^{25}$ −0.9 (*c* 0.5, MeOH). Its molecular formula of $C_{45}H_{67}NO_{11}$ was suggested from a deprotonated high-resolution electrospray ionization mass spectrometric (HR-ESIMS) ion peak at *m*/*z* 798.4796 $[M + H]^+$ (calcd for $C_{45}H_{68}NO_{11}$, 798.4787), indicating 12 degrees of unsaturation. Absorptions for NH stretch (3390 cm^{-1}), olefinic (1608 cm^{-1}), and NH bend (1519 cm^{-1}) groups were observed in its IR spectrum. The UV absorption maxima at 220 nm. The ^1H NMR spectrum (Table 1) of **1** showed signals for one olefinic proton at δ_H 5.37 (1H, brs), three oxygenated methine protons at δ_H 3.38 (1H, dd, J = 11.8, 4.4 Hz), 5.11 (1H, dd, J = 11.5, 5.2 Hz), and 6.37 (1H, dd, J = 10.9, 5.1 Hz), a pair of oxygenated methylene protons at δ_H 4.51 (1H, m) and 4.09 (1H, d, J = 10.6 Hz), seven methyl groups at δ_H 1.45, 1.33, 1.30, 1.01, 1.00, 0.95 and 0.82 (each 3H, s), four aromatic protons at δ_H 8.48 (1H, dd, J = 8.4, 1.8 Hz), 7.39 (1H, ddd, J = 7.8, 7.2, 1.8 Hz), 6.67 (1H, dd, J = 7.8, 1.2 Hz), and 6.66 (1H, ddd, J = 8.4, 7.2, 1.2 Hz), and one nitrogenated methyl group at δ_H 2.80 (3H, overlapped). The ^{13}C NMR spectrum (Table 2) exhibited resonances for one carbonyl carbon at δ_C 168.8, two olefinic carbons at δ_C 143.0 and 124.0, and six aromatic carbons at δ_C 152.2, 135.1, 133.4, 115.1, 112.7 and 111.9. ^1H–^1H COSY (Fig. 2) correlations of H-1/H-2/H-3, H-5/H-6/H-7, H-9/H-11/H-12, H-15/H-16, H-18/H-19, H-21/H-22, H-4′/H-5′/H-6′/H-7′ and H-8′/H-9′ were observed in its structure. An observation of ^1H–^{13}C long-range correlations (Fig. 2) of H-24 (δ_H 1.00) to C-3 (δ_C 89.5), C-4 (δ_C 40.0), C-5 (δ_C 56.0) and C-23 (δ_C 28.6), H-25 (δ_H 0.82) to C-1 (δ_C 39.2), C-5 (δ_C 56.0) and C-10 (δ_C 37.2), H-26 (δ_H 0.95) to C-7 (δ_C 33.3), C-8 (δ_C 40.7), C-9 (δ_C 47.5) and C-14 (δ_C 43.5), H-12 (δ_H 5.37) to C-9 (δ_C 47.5), C-14 (δ_C 43.5) and C-18 (δ_C 44.5), H-30 (δ_H 1.30) to C-19 (δ_C 46.7), C-20 (δ_C 32.8), C-21 (δ_C 39.8) and C-29 (δ_C 33.7), and H-22 (δ_H 6.37) to C-17 (δ_C 46.4) enabled the establishment of pentacyclic triterpene skeleton.[34] Further HMBC correlations of H-22 (δ_H 6.37) to C-1′ (δ_C 168.8), H-7′ (δ_H 8.48) to C-1′ (δ_C 168.8), C-3′ (δ_C 152.2) and C-5′ (δ_C 135.1), and H-8′ (δ_H 2.80) to C-3′ (δ_C 152.2) revealed that an anthranilate group was connected to C-22. Comparison of the NMR data with those of (3β,16β,22α)-22-(*N*-methylanthraniloxy)-16,28-dihydroxyolean-12-en-3-yl-3-*O*-β-D-glucopyranosyl-β-D-glucopyranosidur-onic acid isolated from *Gymnema inodorum*,[35] suggested that **1** had the same aglycone moiety. In addition, a group of sugar-proton signals [δ_H 5.03 (d, J = 7.8 Hz, H-1″), 4.14 (dd, J = 9.0, 7.8 Hz, H-2″), 4.31 (dd, J = 9.6, 9.0 Hz, H-3″), 4.52 (dd, J = 9.7, 9.6 Hz, H-4″), 4.64 (d, J = 9.7 Hz, H-5″)] were observed in the ^1H NMR spectra, of which one anomeric proton signal at δ_H 5.03 (d, J = 7.8 Hz) suggested a β-D-linkage

Table 2 ^{13}C-NMR (150 MHz) data for compounds **1–4** and **9**

	δ_C				
No.	**1**[a]	**2**[a]	**3**[a]	**4**[a]	**9**[b]
1	39.2 (t)	39.1 (t)	39.2 (t)	39.2 (t)	38.6 (t)
2	27.1 (t)	27.1 (t)	27.1 (t)	27.1 (t)	30.8 (t)
3	89.5 (d)	89.5 (d)	89.5 (d)	89.5 (d)	71.8 (d)
4	40.0 (s)	40.0 (s)	40.0 (s)	40.0 (s)	42.0 (t)
5	56.0 (d)	56.0 (d)	56.0 (d)	56.0 (d)	144.2 (s)
6	18.8 (t)	18.8 (t)	18.8 (t)	18.8 (t)	122.7 (d)
7	33.3 (t)	33.2 (t)	33.3 (t)	33.3 (t)	68.3 (d)
8	40.7 (s)	40.6 (s)	40.7 (s)	40.7 (s)	76.2 (s)
9	47.5 (d)	47.4 (d)	47.5 (d)	47.5 (d)	38.8 (d)
10	37.2 (s)	37.1 (s)	37.1 (s)	37.1 (s)	37.8 (s)
11	24.3 (t)	24.3 (t)	24.3 (t)	24.3 (t)	25.2 (t)
12	124.0 (d)	124.6 (d)	124.4 (d)	124.5 (d)	73.2 (d)
13	143.0 (s)	142.0 (s)	142.5 (s)	142.5 (s)	58.0 (s)
14	43.5 (s)	43.2 (s)	43.0 (s)	43.0 (s)	87.7 (s)
15	37.6 (t)	37.8 (t)	36.6 (t)	36.6 (t)	33.6 (t)
16	66.0 (d)	67.0 (d)	66.7 (d)	66.7 (d)	33.4 (t)
17	46.4 (s)	48.6 (s)	44.9 (s)	44.9 (s)	86.8 (s)
18	44.5 (d)	43.4 (d)	44.3 (d)	44.3 (d)	10.8 (q)
19	46.7 (t)	46.3 (t)	46.5 (t)	46.5 (t)	19.8 (q)
20	32.8 (s)	37.2 (s)	32.6 (s)	32.6 (s)	75.6 (d)
21	39.8 (t)	76.9 (d)	44.5 (t)	44.5 (t)	15.2 (q)
22	74.0 (d)	74.0 (d)	70.1 (d)	70.0 (d)	
23	28.6 (q)	28.6 (q)	28.6 (q)	28.6 (q)	
24	17.4 (q)	17.4 (q)	17.3 (q)	17.4 (q)	
25	16.1 (q)	16.0 (q)	16.1 (q)	16.1 (q)	
26	17.4 (q)	17.3 (q)	17.6 (q)	17.6 (q)	
27	28.1 (q)	28.0 (q)	28.1 (q)	28.1 (q)	
28	60.1 (t)	60.6 (t)	63.0 (t)	63.7 (t)	
29	33.7 (q)	29.7 (q)	33.8 (q)	33.8 (q)	
30	25.3 (q)	20.3 (q)	25.3 (q)	25.4 (q)	
	Anth	Anth	Anth	Bz	Cin
1′	168.8 (s)	168.9 (s)	169.4 (s)	167.2 (s)	166.6 (s)
2′	112.7 (s)	111.6 (s)	111.7 (s)	131.6 (s)	118.9 (d)
3′	152.2 (s)	152.5 (s)	152.9 (s)	130.1 (d)	144.5 (d)
4′	111.9 (d)	111.8 (d)	111.9 (d)	129.5 (d)	134.4 (s)
5′	135.1 (d)	135.4 (d)	135.5 (d)	133.8 (d)	128.3(d)
6′	115.1 (d)	115.2 (d)	115.2 (d)	129.5 (d)	128.8 (d)
7′	133.4 (d)	133.3 (d)	131.8 (d)	130.1 (d)	130.3 (d)
8′	30.1 (q)	30.0 (q)	29.8 (q)		128.8 (d)
9′					128.3 (d)
	Glucuronopyranosyl methyl ester	Glucuronopyranosyl methyl ester	Glucuronopyranosyl methyl ester	Glucuronopyranosyl methyl ester	Bz
1″	107.8 (d)	107.8 (d)	107.8 (d)	107.8 (d)	164.8 (s)
2″	75.9 (d)	75.9 (d)	75.9 (d)	75.9 (d)	130.2 (s)
3″	78.4 (d)	78.4 (d)	78.4 (d)	78.4 (d)	129.8 (d)
4″	73.7 (d)	73.7 (d)	73.7 (d)	73.7 (d)	128.6 (d)
5″	77.7 (d)	77.7 (d)	77.7 (d)	77.7 (d)	133.2 (d)
6″	171.4 (s)	171.4 (s)	171.4 (s)	171.4 (s)	128.6 (d)
7″	52.5 (q)	52.5 (q)	52.5 (q)	52.5 (q)	129.8 (d)
		Ac			
1‴		171.2 (s)			
2‴		21.1 (q)			

[a] Pyridine-d_5 as solvent. [b] $CDCl_3$ as solvent.

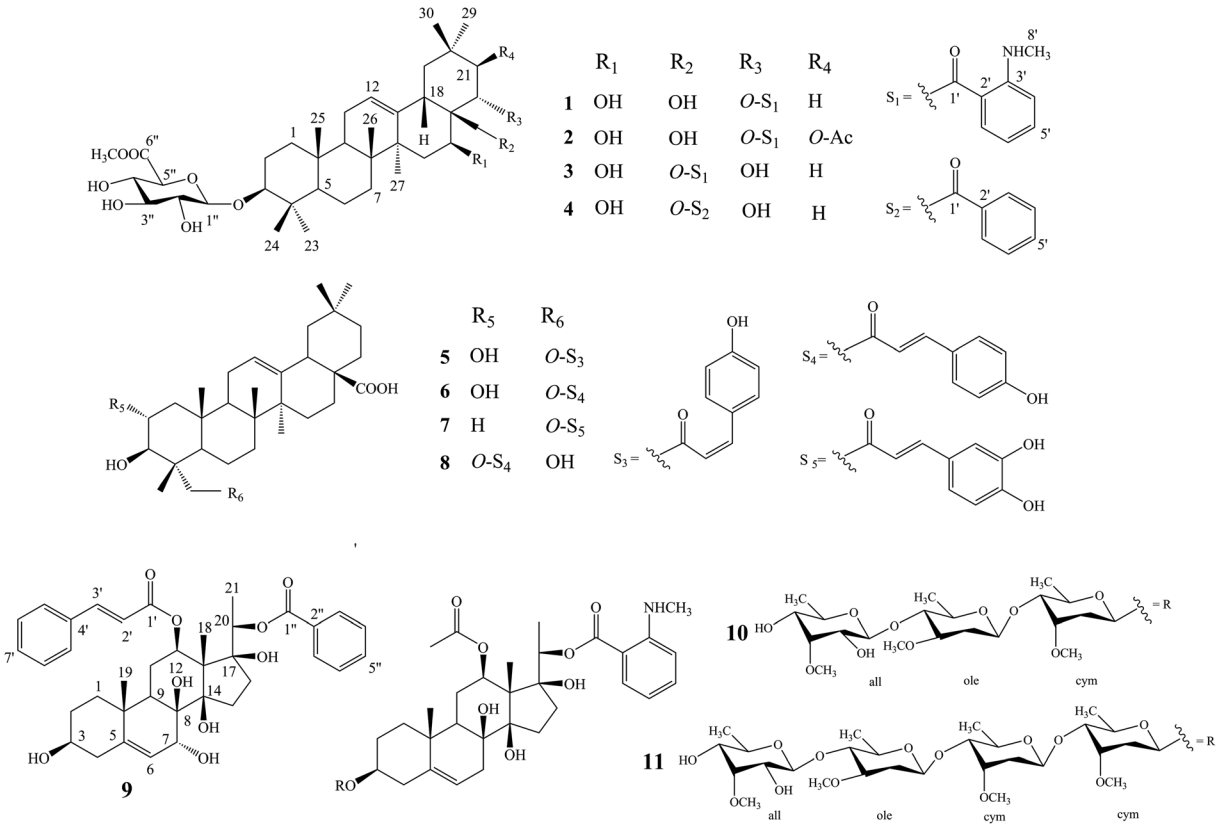

Fig. 1 Structures of compounds **1–11**.

of the sugar moiety in **1**. The HMBC correlations between the carbomethoxyl protons at δ_H 3.75 and the carboxyl group carbon of the glucuronic acid at δ_C 171.4 indicated that glucuronic acid had been methyl esterified. Further analysis of the ^{13}C NMR data of the glycone [δ_C 107.8 (C-1″), 75.9 (C-2″), 78.4 (C-3″), 73.7 (C-4″), 77.7 (C-5″) 171.4 (C-6″), and 52.5 (–OCH_3)] indicated that the glucuronic acid was the same as the sugar moiety of caraganoside C isolated from *Caragana microphylla.*[36] The sugar chain at the C-3 position was indicated by the long-range coupling in the HMBC spectrum of H-3 (δ_H 3.38) to C-1″ (δ_C 107.8). Moreover, the NOESY correlations (Fig. 3) between H-16 (δ_H 5.11) and H-27 (δ_H 1.45) implied that H-16 was α-orientated. The attachment of an anthranilate group at C-22 was deduced as α-oriented based on the NOESY correlation between H-22 (δ_H 6.37) and H-18 (δ_H 3.05). Thus, compound **1** was established as (3β,16β,22α)-22-(*N*-methylanthraniloxy)-16,28-dihydroxyolean-12-en-3-yl-3-*O*-β-D glucuronopyranosyl methyl ester, and named tigensides A.

Compound **2**, a yellow amorphous powder with an $[\alpha]_D^{25}$ +2.4 (*c* 0.5, MeOH), was found to possess a molecular formula of $C_{47}H_{69}NO_{13}$ based on its HRESIMS peak at *m*/*z* 856.4807 [M + H]$^+$ (calcd for $C_{47}H_{70}NO_{13}$, 856.4842), which indicated 13 degrees of unsaturation. The IR spectrum indicated the presence of NH stretch (3433 cm^{-1}) and ester (1743 cm^{-1}) groups. The UV chromatogram of **2** showed maxima absorption at 220 nm. The ^{1}H and ^{13}C NMR data (Tables 1 and 2) of **2** were very similar to those of **1**. The only difference was the presence of signals for an acetyl group at C-21. This was substantiated by means of the observed COSY and HMBC (Fig. 2) correlations of H-21 (δ_H 5.89)/H-22 (δ_H 6.51), H-30 (δ_H 1.34) to C-21 (δ_C 76.9), H-21 (δ_H 5.89) to C-1‴ (δ_C 171.2), and H-2‴ (δ_H 1.89) to C-1‴ (δ_C 171.2). Furthermore, the NOE cross-peaks (Fig. 3) were observed between H-21 (δ_H 5.89) and H-16 (δ_H 5.15), and between H-22 (δ_H 6.51) and H-18 (δ_H 3.16), confirming α-orientation of H-21 and β-orientation of H-22, respectively Thus, compound **2** was assigned as (3β,16β,21β,22α)-22-(*N*-methylanthraniloxy)-21-acetyl- 16,28-dihydroxyolean-12-en-3-yl-3-*O*-β-D glucuronopyranosyl methyl ester, and named tigensides B.

Compound **3** was obtained as a yellow amorphous powder with an $[\alpha]_D^{25}$ +40.9 (*c* 0.5, MeOH). The molecular formula $C_{45}H_{67}NO_{11}$ was determined from the HRESIMS ion peak at *m*/*z* 798.4797 [M + H]$^+$ (calcd for $C_{45}H_{68}NO_{11}$, 798.4787), consistent with 12 degrees of unsaturation. The IR bands at 3390, 1681, and 1519 cm^{-1} were indicative of NH stretch, olefinic, and NH bend groups. The UV chromatogram of **3** indicated the presence of maxima absorption at 220 nm. The ^{1}H and ^{13}C NMR data (Tables 1 and 2) obtained for **3** were very similar to those of **1**. The only observed difference was that the position of an anthranilate group at C-22 in **1** was exchanged to C-28 in **3**. The HMBC correlations (Fig. 2) of H-16 (δ_H 5.17) to C-28 (δ_C 63.0), H-22 (δ_H 4.87) to C-17 (δ_C 44.9), H-28 (δ_H 5.35) to C-17 (δ_C 44.9), C-22 (δ_C 70.1) and C-1′ (δ_C 169.4), and H-30 (δ_H 1.17) to C-21 (δ_C 44.5) indicated that a hydroxyl group was attached to C-22, and an anthranilate group was connected to C-28, which was further

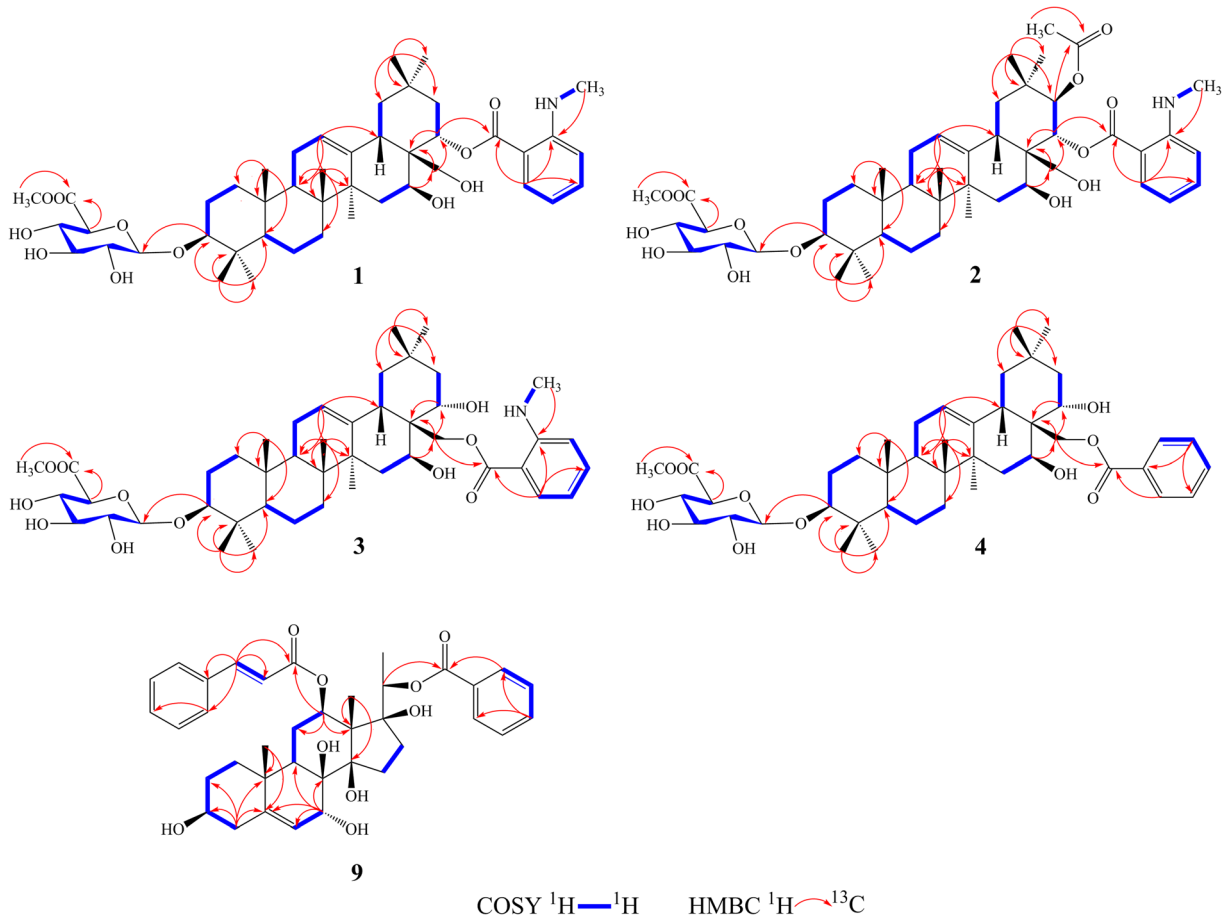

Fig. 2 ^1H–^1H COSY and key HMBC correlations and for compounds **1**–**4** and **9**.

confirmed by its ^1H–^1H COSY correlation (Fig. 2) of H-21 (δ_H 2.11)/H-22 (δ_H 4.86). In addition, the proton on H-22 was determined as β-orientation based on a NOESY correlation (Fig. 3) between H-22 (δ_H 4.86) and H-18 (δ_H 2.95). Thus, the structure of **3** was identified as (3β,16β,22α)-28-(*N*-methylanthraniloxy)-16,22-dihydroxyolean-12-en-3-yl-3-*O*-β-D glucuronopy -ranosyl methyl ester, and named tigensides C.

Compound **4** was obtained as a yellow amorphous powder with an $[\alpha]_D^{25}$ +4.0 (*c* 0.5, MeOH). The molecular formula $C_{44}H_{64}O_{11}$ was determined from the HRESIMS ion peak at *m*/*z* 769.4540 $[M + H]^+$ (calcd for $C_{44}H_{65}O_{11}$, 769.4521), indicating 13 degrees of unsaturation. The IR bands at 3421, 1720, and 1458 cm^{-1} were indicative of the occurrence of hydroxy, ester and olefinic groups. Maxima absorption at 230 nm was observed in the UV chromatogram of **4**. The ^1H and ^{13}C-NMR data (Tables 1 and 2) indicated that the structure of **4** was very similar to **3** except the absence of the signals of the methyl amine group at C-3′ of the aromatic ring. The NMR spectra illustrated typical signals of A_2B_2X system for one benzoyl moiety [δ_H 8.26 (dd, J = 7.8, 2.4 Hz, H-3′/H-7′), δ_C 130.1; δ_H 7.53 (t, J = 7.8 Hz, H-5′), δ_C 133.8; δ_H 7.45 (t, J = 7.8 Hz, H-4′/H-6′), δ_C 129.5]. Furthermore and importantly, the HMBC correlation (Fig. 2) form H-28 (δ_H 5.43) to C-1′ (δ_C 167.2) confirmed the position of the benzoyl group at C-28. Moreover, the configuration of H-22 was characterized as β-orientation based on a NOESY correlation (Fig. 3) between H-22 (δ_H 4.89) and H-18 (δ_H 2.96). Consequently, the structure of compound **4** was established as (3β,16β,22α)-28-*O*-benzoyl-16,22-dihydroxyo -lean-12-en-3-yl-3-*O*-β-D glucuronopyranosyl methyl ester, and named tigensides D.

Compound **9** was obtained as a yellow amorphous powder with an $[\alpha]_D^{25}$ +154.6 (*c* 0.5, MeOH). The molecular formula $C_{37}H_{44}O_9$ was determined from the HRESIMS ion peak at *m*/*z* 633.3062 $[M + H]^+$ (calcd for $C_{37}H_{45}O_9$, 633.3075), consistent with 16 degrees of unsaturation. The IR bands at 3421, 1708 and 1635 cm^{-1} were indicative of the presence of hydroxyl, ester, and olefinic groups. The maxima absorption of **9** was at 220 in the UV chromatogram. The ^1H NMR spectrum (Table 1) demonstrated signals for one olefinic proton δ_H 5.67 (1H, d, J = 4.7 Hz), three methyl groups [δ_H 1.64 (3H, s), 1.36 (3H, d, J = 6.2 Hz), and 1.14 (3H, s)], and four oxygenated methine protons [δ_H 3.60 (1H, m), 4.06 (1H, d, J = 5.2 Hz), 4.86 (1H, overlapped), and 4.91 (1H, d, J = 6.2 Hz)]. Furthermore, the presence of two olefinic carbons (δ_C 144.2 and 122.7), four oxygenated tertiary carbons (δ_C 75.6, 73.2, 71.8, and 68.3), and three oxygenated quaternary carbons (δ_C 87.7, 86.8, and 76.2) in its ^{13}C NMR spectrum suggested the presence of 3,7,8,12,14,17,20-pentahydroxypregnane skeleton.[37] In further support of the skeleton,

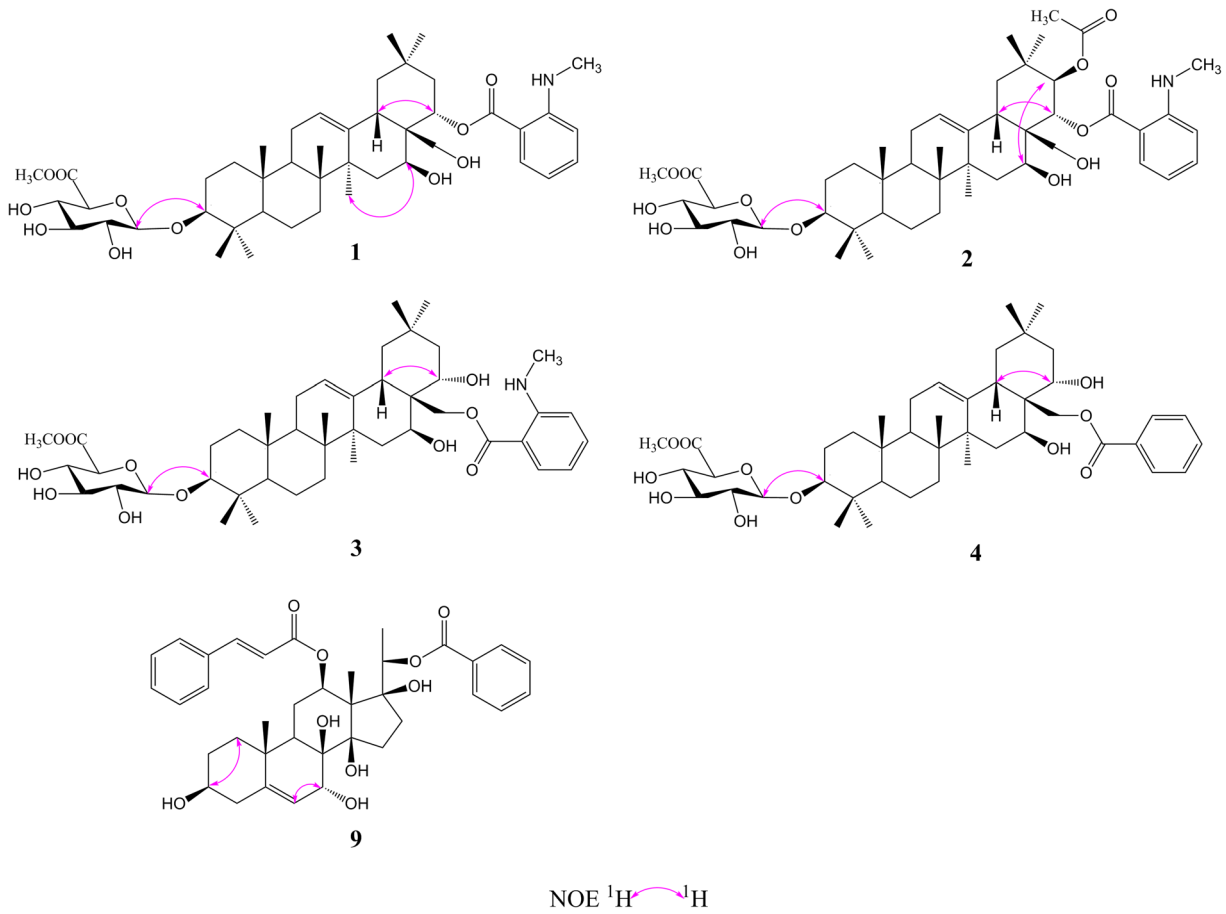

Fig. 3 Key NOE correlations and for compounds **1–4** and **9**.

the following key HMBC correlations (Fig. 2) of δ_H 2.38 (H-4) to 30.8 (C-2), 71.8 (C-3), 144.2 (C-5) and 37.8 (C-10), δ_H 1.14 (H-19) to 144.2 (C-5) and 37.8 (C-10), δ_H 4.06 (H-7) to δ_C 144.2 (C-5), 122.7 (C-6), 76.2 (C-8) and 38.8 (C-9), δ_H 4.86 (H-12) to δ_C 25.2 (C-11) and 58.0 (C-13), and δ_H 1.64 (H-18) to δ_C 58.0 (C-13) and 87.7 (C-14) were observed. The fragments H-1/H-2/H-3/H-4, H-6/H-7, H-9/H-11/H-12, and H-15/H-16 were observed in the ^{1}H–^{1}H COSY spectrum (Fig. 2). In addition, the ^{1}H and ^{13}C NMR data of **9** displayed signals for a benzoyl group [20-Bz: δ_H 7.92 (2H, dd, J = 7.2, 1.5 Hz, H3″/H-7″), 7.56 (1H, t, J = 7.2 Hz, H-5″), and 7.36 (2H, m, H-4″/6″); δ_C 164.8, 133.2, 130.2, 129.8, and 128.6] and a cinnamoyl group [12-Cin: δ_H 7.45 (1H, d, J = 16.0 Hz, H-3′), 7.37 (1H, m, H-7′), 7.33 (2H, m, H-6′/8′), 7.28 (2H, d, J = 7.2 Hz, H-5′/9′), and 6.11 (1H, d, J = 16.0 Hz, H-2′); δ_C 166.6, 144.5, 134.4, 130.3, 128.8, 128.3, and 118.9]. The benzoyl and cinnamoyl groups were located at C-20 and C-12, respectively, by

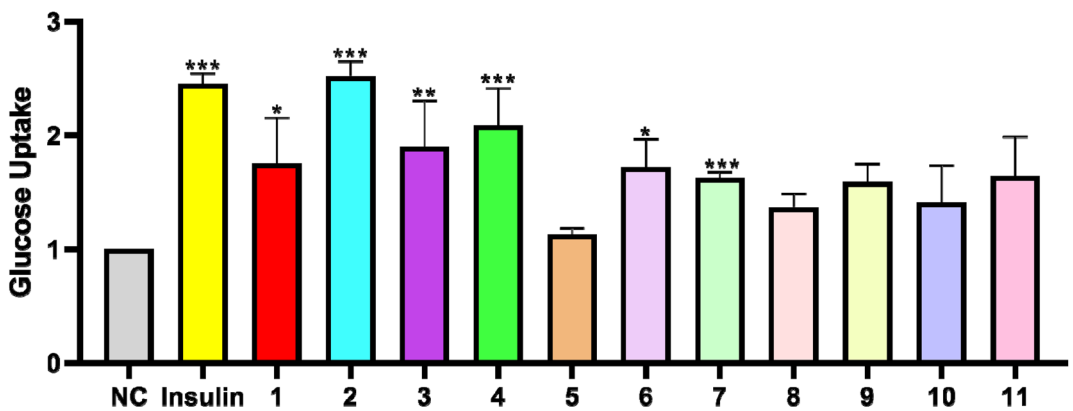

Fig. 4 Effects of compounds **1–11** (30 μg mL^{-1}) on glucose uptake in L6 cells. (*P < 0.05, **P < 0.01, ***P < 0.001, compared with the non-treated group).

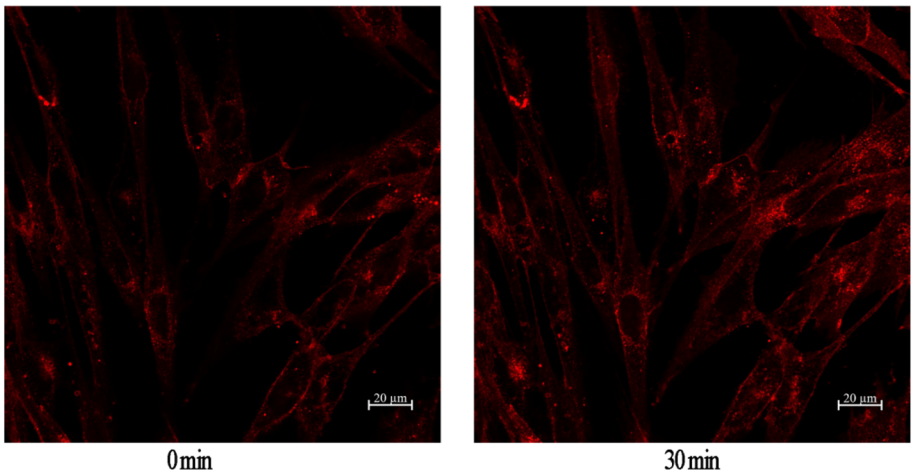

Fig. 5 Effect of compound **2** on GLUT4 translocation in L6 cells.

interpretation of the HMBC correlations of H-20 (δ_H 4.91) to C-1′′ (δ_C 164.8), and H-12 (δ_H 4.86) to C-1′′ (δ_C 166.6). The NMR data of **9** were very similar to those of dibenzoylgagaimol isolated form *Metaplexis japonica* MAKINO.[38] Thus, the structure of **9** was elucidated as 12-*O*-cinnamoyl-20-*O*-benzoyl gagaimol, and named tipregnane **A**.

The other isolated compounds (Fig. 1) were identified as 23-*cis*-*p*-coumaroyloxy-2α,3β-dihydroxyolean-12-en-28-oic acid (**5**),[39] 23-*trans*-*p*-coumaroyloxy-2α,3β-dihydroxyolean-12-en-28-oic acid (**6**),[40] 3β,23-dihydroxy-olean-12-en-28-oic acid 23-caffeate (**7**),[41] tomentoid A (**8**),[42] stephanoside B (**10**),[43] tinctoroside B (**11**),[44] by comparison of their NMR spectra with those of the known compounds.

Glucose uptake assay

Glucose uptake of the tissues and cells is an important link to maintain the stability of blood glucose concentration, and the increase in glucose uptake can improve insulin resistance of T2DM.

In order to test the glucose uptake activity of the isolated compounds, all compounds were selected to evaluate their glucose uptake activity in L6 cells. We treated insulin as the positive control group. Compared with the control group, Compounds **1–11** presented the effects of glucose uptake in L6 cells at 1.12- to 2.52-fold, respectively. Compounds **1**, **3** and **6** exerted weak activity, and showed glucose uptake activity with the enhancement by 1.75-, 1.90-, and 1.72-fold at 30 μg mL^{-1} (Fig. 4). Compounds **4** and **7** possessed a moderate effect on promoting glucose uptake with the enhancement by 2.08- and 1.62-fold at 30 μg mL^{-1}. In addition, compounds **5** and **8** were toxic to L6 cells. Compound **2** was the most active compound, and exhibited glucose uptake activity with 2.52-fold enhancement at 30 μg mL^{-1}.

GLUT-4 translocation assay

GLUT4 is a glucose transporter expressed primarily in adipose and muscle tissues, and is a key regulator of wholebody glucose homeostasis,[45] as its reduced translocation from the intracellular pool to the plasma membranes is reportedly a possible cause of insulin resistance.[46] Therefore there has been considerable interest in targeting GLUT4 for the treatment of T2DM. Based on this target, a cell-based GLUT4 translocation assay using stable L6 cells expressing IRAP-mOrange was established to identify isolated compounds that may have potential antidiabetic effects, by evaluating their effects on the translocation of GLUT4 to the plasma membrane. The confocal microscopy was used to detect IRAP-mOrange trafficking to characterize GLUT4 localization. IRAP, as insulin-regulated aminopeptidase, has been identified as the major protein of GLUT4 storage vesicles (GSVs), which shows strong co-localization with GLUT4 stored in GSVs and may indirectly reflect GLUT4 translocation. The effect of compound **2** on GLUT4 translocation was assessed in L6 cells which stably expressed IRAP-mOrange. As shown in Fig. 5, compound **2** treatment increased fluorescence intensity on L6 cell membranes. The fluorescence reached the greatest intensity (1.36-fold) at 30 minutes after addition of compound **2**. Based on our established GLUT4 translocation assay system, we found that compound **2** displayed a medium effect in promoting GLUT4 translocation and stimulating glucose uptake in L6 cells, indicating that compound **2** possessed potential antidiabetic effects.

Conclusions

In summary, four new triterpenoid saponins (**1–4**) and one new C_{21} steroid (**5**) have been isolated from *G. tingens*, together with six known compounds (**6–11**) in this work. Compounds **1–11** presented the effects of glucose uptake in L6 cells at 1.12- to 2.52-fold, respectively. Specifically, compound **2** exhibited the most potent glucose uptake, with 2.52 – fold enhancement, which was even more potent than the positive control group of insulin. The fluorescence reached the greatest intensity (1.36-fold) at 30 minutes after addition of compound **2**, showing that have a medium effect on the GLUT4 translocation activity in L6 cells in the further study. In addition, the C_{21} steroids show weak activity of glucose uptake. Therefore, triterpenoid

saponins are thought to be the major antidiabetic compounds of *G. tingens*. The study indicates that the separation and characterization of these compounds plays an important role in the research and development of new anti-diabetic phytoconstituents, and the *Gymnema tingens* Spreng. has potential to become a natural resource for developing diabetes drugs.

Experimental section

General experimental procedures

Semi-preparative HPLC purification was performed on a Waters 2535 HPLC connected with a 2998 PDA Detector and a 2707 Autosampler (Waters, Milford, MA, USA). Separations were performed on a COSMOSIL C18 column (5 μm, 10 × 250 mm) (Nacalai Tesque, Kyoto, Japan), a COSMOSIL C8 column (5 μm, 10 × 250 mm) (Nacalai Tesque, Kyoto, Japan) and a YMC-pack diol column (5 μm, 10 × 50 mm; 5 μm, 20 × 150 mm) (Yamamura Chemical Research, Kyoto, Japan). Direct injection high resolution ESIMS and LC-DAD-ESIMS analyses were recorded on an ultra-performance liquid chromatography-quadrupole/electrostatic field orbitrap high resolution mass spectrometry (Thermo Fisher Scientific, Waltham, MA, USA). The NMR spectra were recorded on an AVANCE III 600 MHz spectrometer (Bruker BioSpin, Ettlingen, Germany). Optical rotations were recorded on an Autopol IV Automatic Polarimeter (Rudolph Research Analytical, Hackettstown, NJ, USA). Chromatography grade solvents were used for HPLC, and all other chemical reagents were analytical grade. Sephadex LH-20 dextran gel was purchased from Amersham Pharmacia Biotech Co. (Piscataway, NJ, USA).

Plant materials

The roots and stems of *Gymnema tingens* Spreng. (20191011a) were collected from Guizhou Province, China in October 2019. The roots and stems were identified by Professor Songji Wei of College of Pharmacy, Guangxi University of Chinese Medicine, Nanning, China.

Extraction and isolation

The roots and stems of *G. tingens* (18.2 kg) were exhaustively extracted with 80% aqueous EtOH (2 times × 200 L, each 3 h) at reflux, and the EtOH extract was concentrated to dryness under reduced pressure. The obtained residue (2521.4 g) was suspended in H_2O and partitioned with petroleum ether (PE) (8 × 3.5 L), ethyl acetate (EtOAc) (10 × 3.5 L), and *n*-butyl alcohol (*n*-BuOH) (15 × 3.5 L) to afford 12.2 g of PE fraction, 292.2 g of EtOAc fraction, and 1104.5 g of *n*-BuOH fraction after evaporation, respectively. The EtOAc fraction (292.2 g) was separated on an HP-20 macroporous resin column eluted with EtOH–H_2O (from 0 to 95%, v/v) to give seven fractions Fr.1–Fr.7. Fr.5 (85.1 g) was subjected to silica-gel chromatography column (CC), eluted with a gradient of CH_2Cl_2–CH_3OH (from 200 : 1 to 1 : 1, v/v) to afford eight fractions Fr.5.1–Fr.5.8. Fr.5.4 (35.0 g) was separated into two fractions (Fr.5.4.1, Fr.5.4.2) over silica gel CC with CH_2Cl_2–CH_3OH (from 200 : 1 to 50 : 1, v/v) as the eluent. Fr.5.4.2 (14.8 g) was subjected to an RP-18 column that was eluted with MeOH–H_2O (from 40% to 100%, v/v) to obtain two subfractions Fr.5.4.2.1–Fr.5.4.2.2. Fr.5.4.2.2 (9.0 g) was chromatographed *via* a Sephadex LH-20 column with MeOH as solvent to give two subfractions Fr.5.4.2.2.1 and Fr.5.4.2.2.2. Compounds **10** (13.7 mg) and **11** (17.9 mg) were isolated from Fr.5.4.2.2.1 using semipreparative normal-phase HPLC [*n*-hexane-(*n*-hexaneiso : propyl alcohol, 7 : 3), 15 : 85 to 0 : 100, 9.0 mL min^{-1}, 0 to 30 min] and semipreparative reversed-phase HPLC (MeCN–H_2O, 55 : 45 to 85 : 15, 4.0 mL min^{-1}, 0 to 50 min). Fr.5.5 (7.2 g) was separated by Sephadex LH-20 column (MeOH), and then semipreparative normal-phase HPLC [*n*-hexane-(*n*-hexaneiso : propyl alcohol, 7 : 3), 25 : 75 to 0 : 100, 9.0 mL min^{-1}, 0 to 30 min] to yield seven subfractions Fr.5.5.2.1–Fr.5.5.2.7. Compounds **5** (3.0 mg) and **7** (7.0 mg) were isolated from Fr.5.5.2.3 by semipreparative reversed-phase HPLC (MeCN–H_2O, 40 : 60 to 100 : 0, 4.0 mL min^{-1}, 0 to 20 min). Fr.5.5.2.4 was purified by semipreparative reversed-phase HPLC (MeCN–H_2O, 40 : 60 to 100 : 0, 4.0 mL min^{-1}, 0 to 30 min) to give compounds **6** (76.9 mg) and **8** (10.0 mg). Compounds **1** (23.6 mg), **2** (1.8 mg), **3** (13.8 mg), **4** (26.3 mg), and **9** (7.0 mg) were isolated from Fr.5.5.2.7 by using semipreparative reversed-phase HPLC (MeCN–H_2O, 45 : 55 to 80 : 20, 4.0 mL min^{-1}, 0 to 30 min).

Compound 1. Yellow colour, amorphous powder; $[\alpha]_D^{25}$ −0.9 (*c* 0.5, MeOH); UV (MeOH) λ_{max} (log ε) 220 (1.14) nm; IR (KBr) ν_{max}3390, 2924, 1743, 1681, 1608, 1577, 1519, 1458, 1242, 1172, 1087, 1053, 752, 702 cm^{-1}; HR-ESI-MS (positive): *m*/*z* 798.4796 $[M + H]^+$ (calcd for $C_{45}H_{68}NO_{11}$, 798.4787); NMR data (pyridine-d_5), see Tables 1 and 2.

Compound 2. Yellow colour, amorphous powder; $[\alpha]_D^{25}$ +2.4 (*c* 0.5, MeOH); UV (MeOH) λ_{max} (log ε) 220 (0.21) nm; IR (KBr) ν_{max}3433, 2924, 2357, 1743, 1246, 1172, 1056, 752 cm^{-1}; HR-ESI-MS (positive): *m*/*z* 856.4807 $[M + H]^+$ (calcd for $C_{47}H_{70}NO_{13}$, 856.4842); NMR data (pyridine-d_5), see Tables 1 and 2.

Compound 3. Yellow colour, amorphous powder; $[\alpha]_D^{25}$ +40.9 (*c* 0.5, MeOH); UV (MeOH) λ_{max} (log ε) 220 (1.79) nm; IR (KBr) ν_{max}3390, 2951, 2924, 1743, 1681, 1581, 1519, 1458, 1330, 1242, 1172, 1130, 1087, 1049, 748, 702 cm^{-1}; HR-ESI-MS (positive): *m*/*z* 798.4797 $[M + H]^+$ (calcd for $C_{45}H_{68}NO_{11}$, 798.4787); NMR data (pyridine-d_5), see Tables 1 and 2.

Compound 4. Yellow colour, amorphous powder; $[\alpha]_D^{25}$ + 4.0 (*c* 0.5, MeOH); UV (MeOH) λ_{max} (log ε) 230 (0.55) nm; IR (KBr) ν_{max}3421, 2951, 1720, 1458, 1377, 1276, 1172, 1049, 713 cm^{-1}; HR-ESI-MS (positive): *m*/*z* 769.4540 $[M + H]^+$ (calcd for $C_{44}H_{65}O_{11}$, 769.4521); NMR data (pyridine-d_5), see Tables 1 and 2.

Compound 9. Yellow colour, amorphous powder; $[\alpha]_D^{25}$ +154.6 (*c* 0.5, MeOH); UV (MeOH) λ_{max} (log ε) 220 (1.87) nm; IR (KBr)ν_{max} 3421, 2931, 1708, 1635, 1450, 1280, 1176, 1072, 987, 771, 713 cm^{-1}; HR-ESI-MS (positive): *m*/*z* 633.3062 $[M + H]^+$ (calcd for $C_{37}H_{45}O_9$, 633.3075); NMR data ($CDCl_3$), see Tables 1 and 2.

Glucose uptake and GLUT-4 translocation

Cell culture. L6 cells were added with the prepared whole medium after they were resuscitated and then cultured in

a humidified incubator with 37 °C, ambient oxygen, and 5% CO_2. When the cells grew to about 80%, they were replaced with a differentiation medium and continued to differentiate into myotubes at 37 °C and 5% CO_2 for one week. The medium was changed every 2 days, and the medium was still a differentiation medium. The whole medium was MEM-α (Hyclone, USA) medium containing 10% fetal bovine serum (FBS, Hyclone, USA) and 1% antibiotics (100 U mL^{-1} penicillin and 100 μg mL^{-1} streptomycin), and the differentiation medium was MEM-α medium containing 2% fetal bovine serum and 1% antibiotics.[47,48]

Glucose uptake assay. We used a cell-based fluorescently-labeled deoxyglucose analog kit (2-NBDG kit, Cayman Chemical, USA) to evaluate whether compounds **1–11** increased glucose uptake in L6 cells.[49,50] Before the experiment, the differentiated L6 myotube was inoculated into a 96-well plate at a density of 1×10^4–4×10^4 cells/well. After 2 h of starvation in serum-free α-MEM medium, we add 100 μL MEM-α medium, which contained different drugs, to each well, and cells were incubated for 12 h to 100% fusion. After overnight incubation, cells were treated with insulin (100 nM), compounds **1–11** (30 μg mL^{-1}) or normal control (0.1% DMSO) in 100 μL glucose-free α-MEM containing 150 μg mL^{-1} 2-NBDG. At the end of the treatment, plates were centrifuged for five minutes at 400 g at room temperature. The supernatant was aspirated, and 200 μL of cell-based assay buffer was added to each well. Plates were centrifuged for five minutes at 400 g at room temperature. Then the supernatant was aspirated, and 100 μL of cell-based assay buffer was added to each well. The 2-NBDG taken up by cells was detected with fluorescent filters (excitation/emission = 485/535 nm).

GLUT-4 translocation assay. Construction of myc-GLUT4-mOrange plasmid and cell line were according to the previous report.[51,52] Myc-GLUT4-mOrange-L6 cells were cultured on glass coverslips for 12 h, and then L6 myoblasts are differentiated to L6 myotubes. Cells were starved in a PSS solution for 2 h. After starvation, mOrange fluorescence was detected by laser-scanning confocal microscopy at an excitation wavelength of 555 nm. Cells were treated with 10 μg mL^{-1} tested samples and images were taken every 5 min over a period of 30 min. Zen 2010 Software (Carl Zeiss, Jena, Germany) was used to analyze the fluorescence intensity of mOrange. The detailed method of GLUT4 fusion with the plasma membrane was described as previous reports.

Statistical analysis

The data were shown by means ± standard error of the mean (SEM). One-way analysis of variance (ANOVA) was used to analyse differences between groups, followed by Tukey's post hoc test using Graphpad prime software. A p value of < 0.05 was considered as the levels of statistical significance.

Conflicts of interest

The authors declare that they have no conflict of interest.

Acknowledgements

We are grateful to Prof. Song-Ji Wei of Guangxi University of Chinese medicine, for the identification of the plant. This work was supported by the National Natural Science Foundation of China (No. 81860750) and Inheritance and innovation team of Guangxi Traditional Chinese Medicine (2022B005).

Notes and references

1 F. M. Ashcroft and P. Rorsman, *Cell*, 2012, **148**, 1160–1171.
2 A. Ranjan, R. K. Singh, S. Khare, R. Tripathi, K. Pandey, A. K. Singh, V. Gautam, J. S. Tripathi and S. K. Singh, *Sci. Rep.*, 2019, **9**, 1–13.
3 Y. Li, Y. Liu, J. Liang, T. Wang, M. Sun and Z. Zhang, *J. Agric. Food Chem.*, 2019, **67**, 13051–13060.
4 C. Bommer, V. Sagalova, E. Heesemann, J. M. Goehler, R. Atun, T. Bärnighausen, J. Davies and S. Vollmer, *Diabetes care*, 2018, **41**, 963–970.
5 O. O. Elekofehinti, *Pathophysiology*, 2015, **22**, 95–103.
6 M. Y. Liu, T. X. Zhou, J. Y. Zhang, G. F. Liao, R. M. Lu and X. Z. Yang, *Molecules*, 2021, **26**, 6549.
7 Y. Jiang, B. T. Li, *Flora of China*, Science Press, Beijing, 1977, vol 63, p. 415.
8 G. D. Fabio, V. Romanucci, A. D. Marco and A. Zarrelli, *Molecules*, 2014, **19**, 10956–10981.
9 N. P. Sahu, S. B. Mahato, S. K. Sarkar and G. Poddar, *Phytochemistry*, 1996, **41**, 1181–1185.
10 K. Yoshikawa, K. Matsuchika, K. Takahashi, M. Tanaka, S. Arihara, H. C. Chang and J. D. Wang, *Chem. Pharm. Bull.*, 1999, **47**, 798–804.
11 X. Liu, W. C. Ye, B. Yu, S. X. Zhao, H. M. Wu and C. T. Che, *Carbohydr. Res.*, 2004, **339**, 891–895.
12 K. Kamei, R. Takano, A. Miyasaka, T. Imoto and S. Hara, *J. Biochem.*, 1992, **111**, 109–112.
13 X. Y. Wu, G. H. Mao, Q. Y. Fan, T. Zhao, J. L. Zhao, F. Li and L. Q. Yang, *Food Res. J.*, 2012, **48**, 935–939.
14 S. Vats and R. Kamal, *Pak. J. Biol. Sci.*, 2013, **16**, 1771–1775.
15 P. Nagella, I. M. Chung and H. N. Murthy, *Methods Mol. Biol.*, 2011, **11**, 537–540.
16 P. V. Diwan, I. Margaret and S. Ramakrishna, *Inflammopharmacology*, 1995, **3**, 271–277.
17 S. N. Sinha, G. C. Saha and M. Biswas, *Adv. Biores.*, 2010, **125**, 28.
18 J. K. Malik, F. V. Manvi, B. K. Nanjwade and D. K. Dwivedi, *Der Pharm. Lett.*, 2010, **2**, 336–341.
19 P. Daisy, J. Eliza and K. A. M. M. Farook, *J. Ethnopharmacol.*, 2019, **126**, 339–344.
20 K. M. Ramkuma, C. Manjula, B. Elango, K. Krishnamurthi, S. S. Devi and P. Rajaguru, *Cell Proliferation*, 2013, **46**, 263–271.
21 S. Kumar, P. Gupta, S. Sharma and D. Kumar, *Chin. J. Integr. Med.*, 2011, **9**, 117–128.
22 S. S. Gupta, C. B. Seth and M. C. Variyar, *J. Med. Res.*, 1962, **50**, 73–81.
23 B. Anupam and C. H. Malay, *Phytother. Res.*, 1994, **8**, 118–120.

24 M. Yoshikawa, T. Murakami, M. Kadoya, Y. H. Li, N. Murakami, J. Yamahara and H. Matsuda, *Chem. Pharm. Bull.*, 1997, **45**, 1671–1676.
25 K. Shimizu, A. Iino, J. Nakajima, K. Tanaka, S. Nakajyo, N. Urakawa, M. Atsuchi, T. Wada and C. Yamashita, *J. Vet. Med. Sci.*, 1997, **59**, 245–251.
26 S. Yoshioka, T. Imoto, M. Miyoshi, T. Kasagi, R. Kawahara and Y. Hiji, *WakanIyaku Zasshi*, 1996, **13**, 300–303.
27 M. Yoshikawa, T. Murakami and H. Matsuda, *Chem. Pharm. Bull.*, 1997, **45**, 2034–2038.
28 H. J. H. Kahksha, O. Alam, S. Naaz, V. Sharma, A. Manaithiya, J. Khan and A. Alam, *J. Ethnopharmacol.*, 2020, **286**, 114908.
29 Y. Jiang and B. T. Li, *Flora of China*, Science Press, Beijing, 1977, vol 63, p. 422.
30 D. P. Khare, A. Khare and M. P. Khare, *Carbohydr. Res.*, 1980, **81**, 285–294.
31 J. C. He, M. Y. Wang and Z. C. Dong, *Nat. Prod. Res. Dev.*, 2013, **25**, 1673–1675.
32 J. Tian, *Studies on Chemical Constituents of Gymnema tingens*, Peking Union Medical College, 2013.
33 Y. Huang, J. Hao, D. Tian, Y. Z. Wen, P. Zhao, H. Chen, Y. B. Lv and X. Z. Yang, *Front. Pharmacol.*, 2018, **9**, 760.
34 J. L. Li, J. Zhou, Z. H. Chen, S. Y. Guo, C. Q. Li and W. M. Zhao, *J. Nat. Prod.*, 2015, **78**, 1548–1555.
35 J. P. An, E. J. Park, B. Ryu, B. W. Lee, H. M. Cho, T. P. Doan, T. T. Pham and W. K. Oh, *J. Nat. Prod.*, 2020, **83**, 1265–1274.
36 G. L. Jin, C. J. Zheng, W. B. Xin, Z. J. Mao, P. X. Sun, Z. X. Zeng and L. P. Qin, *Arch. Pharmacal Res.*, 2011, **34**, 869–873.
37 M. A. Raees, H. Hussain, A. A. Rawahi, R. Csuk, A. A. Ghafri, N. U. Rehman, A. Elyassi, I. R. Green, T. Mahmood and A. A. Harrasi, *Phytochem. Lett.*, 2016, **16**, 230–235.
38 T. Nomura, T. Fukai and T. Kuramochi, *Planta Med.*, 1981, **41**, 206–207.
39 J. Xiong, Y. Huang, Y. Tang, M. You and J. F. Hu, *Chinese J. Org. Chem.*, 2013, **33**, 1304–1308.
40 J. Q. Gu, E. J. Park, L. Luyengi, M. E. Hawthorne, R. G. Mehta, N. R. Farnsworth, J. M. Pezzuto and A. D. Kinghorn, *Phytochemistry*, 2001, **58**, 121–127.
41 H. Pan, L. N. Lundgren and R. Andersson, *Phytochemistry*, 1994, **37**, 795–799.
42 Y. B. Zhang, W. Li, Z. M. Zhang, N. H. Chen, X. Q. Zhang, J. W. Jiang, G. C. Wang and Y. L. Li, *Chem. Lett.*, 2016, **45**, 368–370.
43 K. Yoshikawa, N. Okada, Y. Kann and S. Arihara, *Chem. Pharm. Bull.*, 1996, **44**, 1790–1796.
44 Z. L. Gao, H. P. He, Y. T. Di, X. Fang, C. S. Li, Q. Zhang, P. J. Zhao, S. L. Li and X. J. Hao, *Helv. Chim. Acta*, 2009, **92**, 1775–1781.
45 S. Yonemitsu, H. Nishimura, M. Shintani, R. Inoue, Y. Yamamoto, H. Masuzaki, Y. Ogawa, K. Hosoda, G. Inoue, T. Hayashi and K. Nakao, *Diabetes*, 2001, **50**, 1093–1101.
46 D. Leto and A. R. Saltiel, *Nat. Rev. Mol. Cell Biol.*, 2012, **13**, 383–396.
47 R. J. Koenig and R. J. Smith, *J. Clin. Invest.*, 1985, **76**, 878–881.
48 Q. Zhou, X. Yang, M. Xiong, X. Xu, L. Zhen, W. Chen, Y. Wang, J. Shen, P. Zhao and Q. H. Liu, *Cell. Physiol. Biochem.*, 2016, **38**, 2030–2040.
49 Y. Huang, T. Zhou, Y. Zhang, H. Huang, Y. Ma, C. Wu, C. Wang, Q. Lin, X. Yang and K. Pang, *J. Funct. Foods*, 2021, **77**, 104338.
50 G. Song, Y. Huang, M. Xiong, Z. Yang, Q. Liu, J. Shen, P. Zhao and X. Yang, *Front. Pharmacol.*, 2021, **11**, 561956.
51 Y. Lv, P. Zhao, K. Pang, Y. Ma, H. Huang, T. Zhou and X. Yang, *J. Ethnopharmacol.*, 2021, **268**, 113654.
52 Y. Ma, T. Zhou, P. Zhao, H. Y. Choi, J. Hao, H. Huang, C. Wu, X. Yang and K. Pang, *Bioorg. Chem.*, 2021, **106**, 104500.